Journal of Muscle Research and Cell Motility **22**: 467–475, 2001.

Tibialis anterior muscles in *mdx* mice are highly susceptible to contraction-induced injury

CHRISTIANA DELLORUSSO[1,2,4], ROBERT W. CRAWFORD[1,4], JEFFREY S. CHAMBERLAIN[1,4] and SUSAN V. BROOKS[2,3,*]

[1]*Departments of Human Genetics and* [2]*Physiology;* [3]*Institute of Gerontology, University of Michigan, 300 North Ingalls Building, Ann Arbor, Michigan 48109-2007, USA*

Received 24 May 2001; accepted in revised form 26 September 2001

Abstract

Skeletal muscles of patients with Duchenne muscular dystrophy (DMD) and *mdx* mice lack dystrophin and are more susceptible to contraction-induced injury than control muscles. Our purpose was to develop an assay based on the high susceptibility to injury of limb muscles in *mdx* mice for use in evaluating therapeutic interventions. The assay involved two stretches of maximally activated tibialis anterior (TA) muscles *in situ*. Stretches of 40% strain relative to muscle fiber length were initiated from the plateau of isometric contractions. The magnitude of damage was assessed one minute later by the deficit in isometric force. At all ages (2–19 months), force deficits were four- to seven-fold higher for muscles in *mdx* compared with control mice. For control muscles, force deficits were unrelated to age, whereas force deficits increased dramatically for muscles in *mdx* mice after 8 months of age. The increase in susceptibility to injury of muscles from older *mdx* mice did not parallel similar adverse effects on muscle mass or force production. The *in situ* stretch protocol of TA muscles provides a valuable assay for investigations of the mechanisms of injury in dystrophic muscle and to test therapeutic interventions for reversing DMD.

Introduction

Duchenne muscular dystrophy (DMD), a lethal X-linked recessive disorder that affects one in 3500 newborn males, is the most common form of childhood muscular dystrophy (Emery, 1993). The disease is characterized by a progressive loss of muscle strength and the replacement of muscle by fat and connective tissue. DMD patients have mutations in the gene for the subsarcolemmal protein dystrophin (Hoffman *et al.*, 1987). As is the case for DMD patients, *mdx* mice lack dystrophin (Bulfield *et al.*, 1984; Sicinski *et al.*, 1989) and mimic the human disease genetically and biochemically. The exact function of dystrophin is unclear, but it appears to aid in maintenance of muscle fiber membrane integrity in both quiescent and contracting muscles (Petrof *et al.*, 1993; Straub *et al.*, 1997; Lynch *et al.*, 2000). Unlike the wasting of muscle in DMD patients, to which they succumb in the second or third decade of life, limb muscles in *mdx* mice exhibit a compensatory hypertrophy that maintains absolute force production at or above control values throughout the life span (Sacco *et al.*, 1992; Faulkner *et al.*, 1997; Lynch *et al.*, 2001). The compensatory hypertrophy appears to result from the maintenance of a regenerative process that does not persist in DMD patients or in the diaphragm muscles of *mdx* mice (Stedman *et al.*, 1991). Although force is maintained in the limb muscles of *mdx* mice, the lack of dystrophin results in increased susceptibility to contraction-induced injury (Moens *et al.*, 1993; Petrof *et al.*, 1993; Brooks, 1998). This type of injury, induced through lengthening contractions that stretch activated muscles, is potentially a mechanism for the progression of muscular dystrophy and the loss of regenerative capacity in the muscles of DMD patients (Petrof *et al.*, 1993).

The high frequency and lethality of DMD, in addition to the availability of cloned genes and animal models, make DMD a candidate disease for gene therapy (Hartigan-O'Connor and Chamberlain, 2000). The delivery of potentially therapeutic agents to mouse muscle is crucial in determining the success of preventing or reversing muscular dystrophy (Cox *et al.*, 1993; Phelps *et al.*, 1995). While diaphragm muscles in *mdx* mice are an excellent model for DMD, both access to the muscle for intervention and the ability to analyze only small strips of muscle fibers rather than the entire muscle present major experimental complications. In contrast, the tibialis anterior (TA) muscle is located in the anterior compartment of the lower hind limb and is in ideal position for needle injections and functional testing in its entirety. The extensive use of the TA muscle in injection experiments testing therapeutic agents (Gilbert *et al.*, 1999; Greelish *et al.*, 1999; Ebihara *et al.*, 2000; Ferrer *et al.*, 2000; Wakefield *et al.*, 2000; Byun *et al.*, 2001) provides a

* To whom correspondence should be addressed: Tel.: +1-734-9362147; Fax: +1-734-9362116; E-mail: svbrooks@umich.edu

[4] Current address: Department of Neurology, University of Washington, Seattle, WA 98195-7720.

powerful rationale for the significance of defining a sensitive assay to evaluate the efficacy of a treatment.

Our purpose was to develop a contraction-induced injury protocol that reveals the high susceptibility of TA muscles in *mdx* compared with control mice to injury and thereby provides a useful assay for studying the effectiveness of gene therapy interventions. A decrease in the susceptibility to contraction-induced injury may prevent or reverse the progression of dystrophy, even if such gene transfer does not result in the restoration of normal force or power development. We studied mice 2–19 months of age, as we are interested not only in the potential to prevent the progressive loss of muscle function with age, but also the ability of delivered therapeutic agents to reverse muscular dystrophy in affected muscles. The TA muscle injured *in situ* provides an assay that allows precise and reproducible measurements without removing the muscle from its natural environment. The assay was also designed to enable the use of the deficit in force immediately following the injury-inducing protocol as a measure of damage without fatigue as an additional factor in the loss of force generating capacity.

Materials and methods

Animals

Mice aged 2–19 months were tested. Specific pathogen free (SPF) C57BL control and *mdx* mice were either purchased or bred in-house with mating pairs purchased from the Jackson Laboratories. All control mice were of C57BL/10J strain with the exception of the 19-month-old mice that were C57BL/6. The use of C57BL/6 mice for the oldest group was necessary, since unlike C57BL/10J mice, C57BL/6 mice may be purchased at advanced ages from the colonies of aging rodents maintained by the National Institute on Aging. Mice were housed until reaching the appropriate age in a SPF-barrier facility in the University of Michigan Unit for Laboratory Animal Medicine. All protocols were performed in accordance with the guidelines of the University of Michigan's Committee on the Use and Care of Animals and the USPHS Guide for the Care and Use of Laboratory Animals (DHHS Pub. no. 85-23 (NIH), Revised 1985, Office of Science and Health reports, Bethesda, MD).

In situ *preparation*

Mice were anesthetized with an initial intraperitoneal injection of Avertin (tribromoethanol; 13–17 μl/g). Anesthesia was supplemented until no responses to tactile stimuli were detected. This level of anesthesia was maintained throughout the experiment with additional doses of Avertin. The tendon of the TA was exposed by an incision at the ankle. The tendon was cut several millimeters distal to the end of the muscle. The tendon was tied with 4.0 nylon suture as close to the muscle attachment as possible, and the tendon was folded back onto itself and tied again. The tendon and exposed muscle were kept moist by periodic applications of isotonic saline. The mouse was placed on a heated platform maintained at 37°C. The foot of the mouse was secured to the platform with cloth tape and the knee was immobilized in a Plexiglas™ clamp between sharpened screws. The tendon of the muscle was tied securely to the lever arm of a servomotor (Model 305B-LR, Aurora Scientific, Richmond Hill, ON, Canada). The servomotor controlled the position of the muscle and monitored the force developed by the muscle. All data were displayed on a digital oscilloscope (Gould, model 475) and stored on a computer.

The TA muscle was stimulated with 0.2-ms pulses (Grass, model S88) via two needle electrodes that penetrated the skin on either side of the peroneal nerve near the knee. Stimulation voltage and subsequently muscle length (L_o) were adjusted for maximum isometric twitch force (P_t). While held at L_o, the muscle was stimulated at increasing frequencies, stepwise from 150 Hz by 50 Hz, until a maximum force (P_o) was reached, typically at 250 Hz. A one- to two-minute rest period was allowed between each tetanic contraction. Muscle length was measured with calipers, based on well-defined anatomical landmarks near the knee and the ankle. Optimum fiber length (L_f; see Table 1) was determined by multiplying L_o by the TA L_f/L_o ratio of 0.6 (Burkholder *et al.*, 1994).

Lengthening contraction protocol

Each muscle was exposed to two stretches *in situ*, with the muscle stimulated at 250 Hz, the frequency that most often resulted in P_o. A protocol consisting of only two contractions was used to avoid fatigue. Stretches were initiated from the plateau of an isometric contraction at L_o. The time course of the protocol is shown in Figure 1. At time 0, stimulation was initiated and the muscle was held with no movement for 100 ms to allow maximum activation. From the plateau of the maximum isometric contraction, a length change of 40% L_f at a velocity of 2 L_f/s was imposed (LC1). Stimulation ceased at the end of the stretch ramp. The muscle was held at the stretched length for 100 ms and then returned to L_o at the same velocity. A second lengthening contraction identical to the first was administered 10 s later (LC2). Maximum isometric force was measured after 1 min (+1 min) and then again each 5 min for 15 min. Force deficits were calculated as the difference between the isometric force during LC1 and the maximum isometric force measured at any given time and expressed as a percentage of the isometric force during LC1. The recovery during the 15 min following the two-lengthening-contraction protocol was quantified as the difference between the isometric force measured at 15 min and the isometric force after the second lengthening contraction and expressed as a percentage of initial P_o.

Table 1. Body masses and tibialis anterior (TA) muscle fiber lengths for *mdx* and control (C57BL) mice 2–19 months of age

Age (months)	Number of mice	Body mass (g)	Number of TA muscles	L_f (mm)
mdx				
2–3	3	29.0 ± 0.6	6	6.6 ± 0.1
4–6	4	34.0 ± 1.2	6	6.6 ± 0.1
6–8	6	34.7 ± 0.8[a]	9	6.5 ± 0.2
11–13	7	34.5 ± 1.0	8	7.1 ± 0.2
19	4	29.8 ± 0.8	7	6.5 ± 0.1
C57BL				
2–3	3	26.7 ± 0.7	5	6.2 ± 0.1
4–6	6	31.2 ± 1.3	8	6.3 ± 0.2
6–8	2	29.5 ± 0.5	4	7.2 ± 0.1
11–13	3	36.0 ± 2.5	6	6.4 ± 0.1
19	3	30.3 ± 0.3	6	6.8 ± 0.1

Shown are the total numbers of mice and TA muscles studied and the mean body masses and mean TA fiber lengths (L_f) for each age group. There was a significant effect of both age ($P < 0.0001$) and strain ($P = 0.049$) on body mass.
[a] A difference between *mdx* and C57BL mice of the same age. The single individual difference demonstrates that the strain effect was weak. There was a significant effect of age ($P = 0.01$) on L_f, but no difference between L_f for muscles from *mdx* and C57BL mice.

After the final evaluation of isometric force, the TA muscle was removed from the mouse. The tendon and suture were trimmed from the muscle, and the muscle was weighed. After removal of TA muscles, deeply anesthetized mice were euthanized by the induction of a pneumothorax. Total muscle fiber cross-sectional area (CSA) of TA muscles was calculated by dividing muscle mass by the product of L_f and 1.06 mg/mm^3, the density of mammalian skeletal muscle (Mendez and Keys, 1960). Specific P_o was calculated by dividing P_o by CSA.

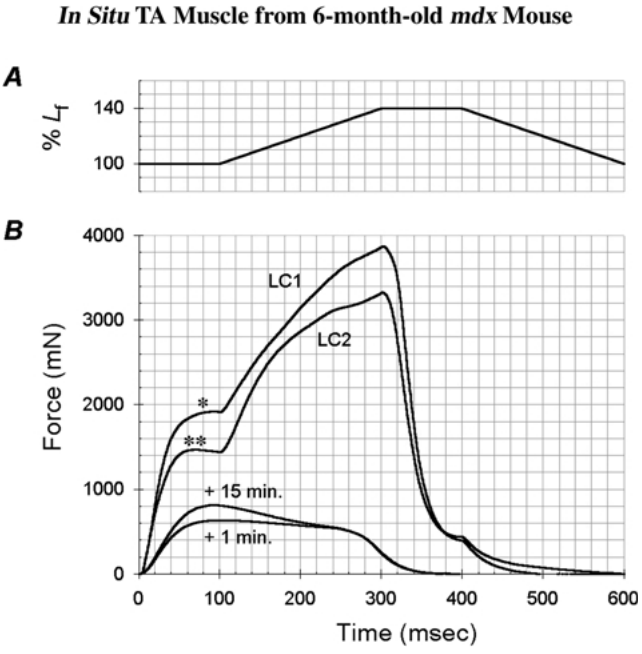

Fig. 1. Lengthening contractions induced muscle injury and decreased P_o. The experimental protocol consisted of two muscle stretches during maximal activation, followed by maximal activation to measure the decrease in maximum isometric force (P_o). Panel A shows the length change of the muscle of 40% strain relative to fiber length (L_f), where 100% corresponds to optimum muscle length (L_o) for force development. The muscle was stretched at a velocity of 2 L_f/s. Panel B demonstrates the decrease in P_o after the two-stretch protocol in a representative *mdx* mouse. Each lengthening contraction was initiated from the plateau of a maximum isometric contraction. Ten seconds after the first lengthening contraction (LC1), a second lengthening contraction occurred (LC2). Maximum force during an isometric contraction was measured 1 min after LC2 (+1 min) and again after 15 min of recovery (+15 min). The force deficit was calculated by dividing the difference between the P_o during LC1 (*) and the P_o measured at any time after LC1 (**, +1 min, +15 min, etc.) by the P_o during LC1 and multiplying by 100%. For example, the calculation for the force deficit after LC1 shown here is ((1912−1441) mN/1912mN) × 100% = 24.6%.

Histology

After obtaining the muscle mass, some TA muscles were cut in half in cross section, oriented midsection up in OCT tissue freezing compound on pieces of cork and frozen rapidly in isopentane cooled with liquid nitrogen. Specimens were kept at −80°C until sectioning. Serial cryosections of 5 μm thickness that had equilibrated to room temperature were stained with either hematoxylin (nuclear stain) and eosin-phloxine (cytoplasmic stain) (H&E), or Alizarin red (sodium alizarin sulfate, calcium ion stain (Bodensteiner and Engel, 1978)). Slides were stained in Alizarin red for 2 min, and then washed 4 × 1 min in acetone, 1 min in 1:1 acetone/xylene, and 2 × 1 min in xylene. Coverslips were positioned on the slides and attached using a drop of Paramount and dried at room temperature overnight before viewing under a light microscope. Serial sections of the TA were fixed in 3.7% formaldehyde and stained with H&E as described previously (Dubowitz, 1985).

To minimize observer bias in determining Alizarin red positive fibers, Image Pro Plus 4.0 software (Media Cybernetics, Silver Spring, MD) was used to estimate the Alizarin red positive area in each cross section. Six 100× representative and random microscopic fields from each muscle cross section were photographed under identical conditions. Each image was analyzed by applying the same brightness and contrast thresholds in Image Pro to capture only the Alizarin red stain and to exclude most background staining. Initial analyses showed no effect of age on the Alizarin red positive

area in either *mdx* or control mice. Consequently, data from different ages were pooled and the average Alizarin red positive area for each case (see Figure 5) was calculated from all of the fields analyzed.

Data analysis

Data are presented as the mean ± the standard error of the mean (SEM). Statistical analyses were performed using Statview software for Macintosh. An initial paired *t*-test was used to test for differences between the right and left TA muscles. No effects of paired muscles were observed, and each TA muscle was treated as an individual case. For both contractile and morphological data, differences between groups were determined by two-way analysis of variance (ANOVA) with strain of mouse (control and *mdx*) and age (groupings: 2–4, 4–6, 6–8, 11–13, and 19 months) as factors. When a positive effect was observed, a Tukey–Kramer post-hoc test was used to determine differences between group means. Significance was assessed in all cases by a *P*-value of ≤ 0.05.

Results

A total of 36 muscles from 24 *mdx* mice and 29 muscles from 17 control mice were examined. Mean body masses and TA *L* for mice in each age group are shown in Table 1. Age had significant effects on both body mass and L_f, however these effects appear to be cohort rather than aging effects, as there were no trends for increasing or decreasing body mass or L_f with age. At only a single age (6–8 months) was there a significant difference in body mass between *mdx* and control mice, and there were no differences between L_f measurements made in TA muscles from the two strains of mice.

Figure 2 displays mean TA muscle masses and forces for all of the muscles studied. No effect of age was observed for TA muscle masses in either *mdx* or control mice. Masses of TA muscles from *mdx* mice were consistently higher than muscles from the age-matched controls with TA muscle masses on average 35% higher in *mdx* mice than in control mice. The P_o for TA muscles from *mdx* mice was also consistently greater than or equal to P_o measured for muscles from control mice. This difference in P_o was significantly greater for TA muscles of *mdx* compared with control mice in the 4–6, 11–13, and 19-month-old age groups. When values of absolute P_o were normalized by CSA of the TA muscles, specific P_o showed significant weakness of 20–25% for muscles from *mdx* compared with control mice across all age groups examined. While age was a significant factor in P_o and specific P_o, like the body mass data, these were more likely cohort rather than aging effects.

In all cases, force deficits were dramatically greater for muscles from *mdx* mice than control mice (Figure 3). For mice 8 months of age or younger, force deficits after

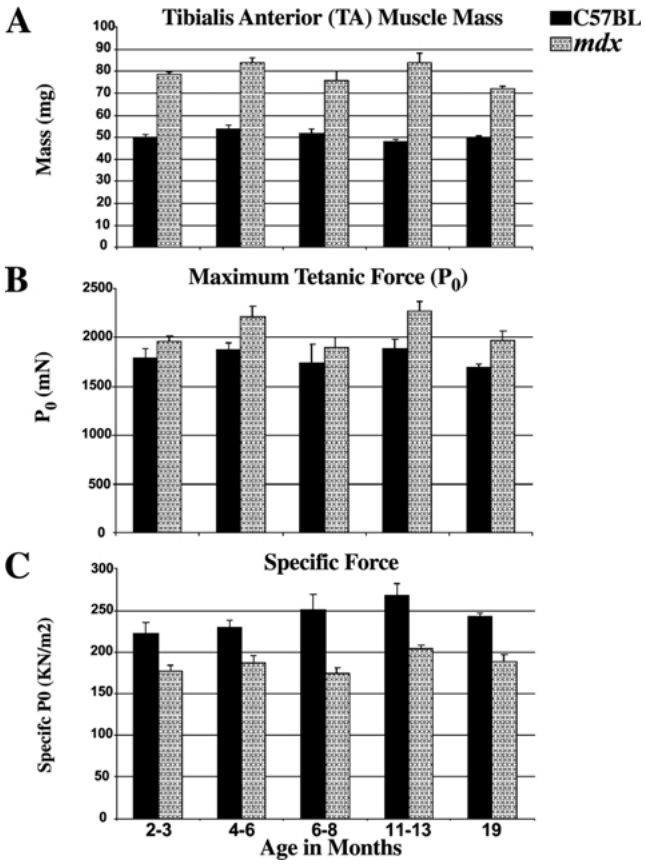

Fig. 2. Hypertrophy and maintenance of force in *mdx* TA muscles accompanied lower specific forces. Panel A shows the masses of TA muscles from *mdx* and control mice. A significant effect of strain ($P < 0.0001$) was observed, with masses of TA muscles of *mdx* mice significantly higher than control muscle masses in all age groups studied. There was no age effect for muscle mass. Panel B reveals both a strain ($P = 0.0001$) and age ($P = 0.03$) effect of maximum isometric tetanic force (P_o). For the strain effect, significant differences between TA muscles from *mdx* and C57BL mice were observed in the 4–6, 11–13, and 19-month-old age groups. When P_o was normalized to muscle cross-sectional area in C, TA muscles from *mdx* mice showed significant weakness compared to muscles from control mice in all age groups studied ($P < 0.0001$). An effect of age was also observed ($P = 0.004$) for specific force.

one lengthening contraction were approximately four-fold greater for muscles from *mdx* compared with control mice, whereas following two lengthening contractions, force deficits from *mdx* mice were seven-fold greater. Interestingly, for TA muscles of *mdx* mice, the force deficits after one lengthening contraction increased markedly between 8 and 11 months from 28 ± 2 to 72 ± 6%. After two lengthening contractions, TA muscles from *mdx* mice 11 months of age or older demonstrated almost a complete inability to generate force with force deficits of 98 ± 1%. In contrast to the increase in susceptibility to damage of TA muscles in the older age groups of *mdx* mice, for muscles in control mice no differences were observed at any age for force deficits following either one or two lengthening contractions. The combination of the greater force deficits for muscles in older *mdx* mice with no change in force deficit with aging for control mice resulted in even

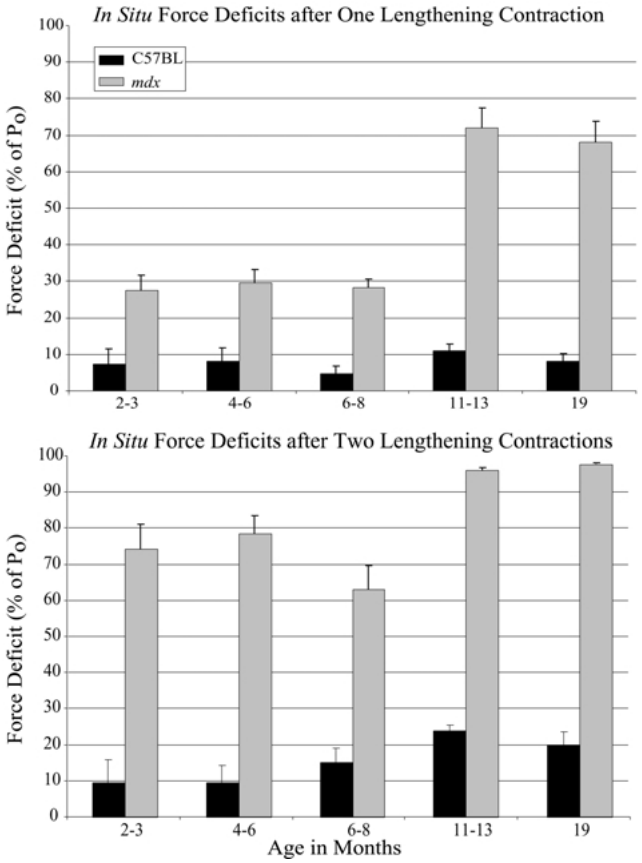

Fig. 3. Force deficits after one and two lengthening contractions were higher in TA muscles from *mdx* mice in all age groups. The force deficits of TA muscles revealed a significant strain effect ($P < 0.0001$) in muscles from *mdx* compared with control mice at all age groups studied after both LC1 and LC2. A significant age effect ($P < 0.0001$) was also observed in TA muscles of *mdx* mice after both LC1 and LC2, as the susceptibility to injury increased dramatically after 8 months of age.

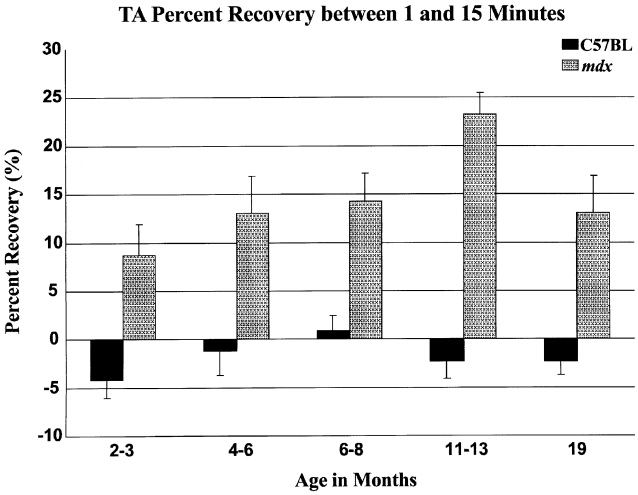

Fig. 4. The injury induced by two lengthening contractions was partially restored after 15 min in *mdx* mice. Percent recovery was calculated as the difference between the isometric force measured at 15 min and the isometric force at 1 min (after LC2), and expressed as a percentage of initial P_o. Age was not a factor in the magnitude of recovery. P_o measurements made after 15 min of recovery showed that TA muscles from control mice did not recover any of the force lost after two lengthening contractions. In contrast, muscles from *mdx* mice showed an average recovery of 15.3 ± 1.6%. For this significant strain effect, $P < 0.0001$.

greater differences between muscles in *mdx* and control mice at the older ages.

TA muscles from control mice of all ages showed no recovery of force during the 15-minute recovery period, as shown in Figure 4. The lack of a change in the force deficit over time observed for muscles of control mice supports no role of fatigue in the force deficits measured for TA muscles following the two-contraction protocol. Furthermore, the lack of change in the force deficit during 15 min following two lengthening contractions shows that the damage in TA muscles from control mice is not quickly recoverable. In contrast, TA muscles in *mdx* mice recovered significantly in the 15 min following the stretches. The magnitude of the recovery tended to increase with age but the effect was not significant. The average recovery of 15 ± 2% of the force deficit after the stretch protocol suggests that at least a portion of the damage to TA muscles in *mdx* mice is rapidly resolved.

Cross sections of TA muscles stained with H&E and Alizarin red are shown in Figure 5. Quantitative analysis revealed a very small amount of Alizarin red positive area in TA muscle sections (0.1% of the total field area) from control mice, with little change in the positive area after the stretch protocol (0.2% of field area). The amount of cross-sectional area that was positive for Alizarin red was greater in muscles from *mdx* mice. In unstretched muscles from *mdx* mice, 2.1% of the total field area was Alizarin red positive, and the Alizarin red positive area increased to 7.4% of total field area after the stretch protocol.

Discussion

The high susceptibility to contraction-induced injury of TA muscles in *mdx* mice observed in the present study is consistent with previous reports on the response of other fast-twitch muscles of *mdx* mice, primarily the extensor digitorum longus (EDL) muscle, to lengthening contractions (Moens *et al.*, 1993; Petrof *et al.*, 1993; Brooks, 1998). Despite the dramatically greater susceptibility to injury observed for TA muscles in *mdx* compared with control mice, as well as the increasing susceptibility to injury with aging in *mdx* mice, muscle hypertrophy and normal levels of absolute force were maintained at all ages studied. The disparity between the effects of dystrophin deficiency on isometric force and susceptibility to injury (present study; Deconinck *et al.*, 1998) illustrates different manifestations of the dystrophic process and emphasizes the importance of examining multiple facets of muscle function. The ability to evaluate the effects of therapeutic agents delivered to muscles of mice is critical for demonstrating successful prevention or reversal of muscular dystrophy (Cox *et al.*, 1993; Phelps *et al.*, 1995). Due in large part to its accessibility

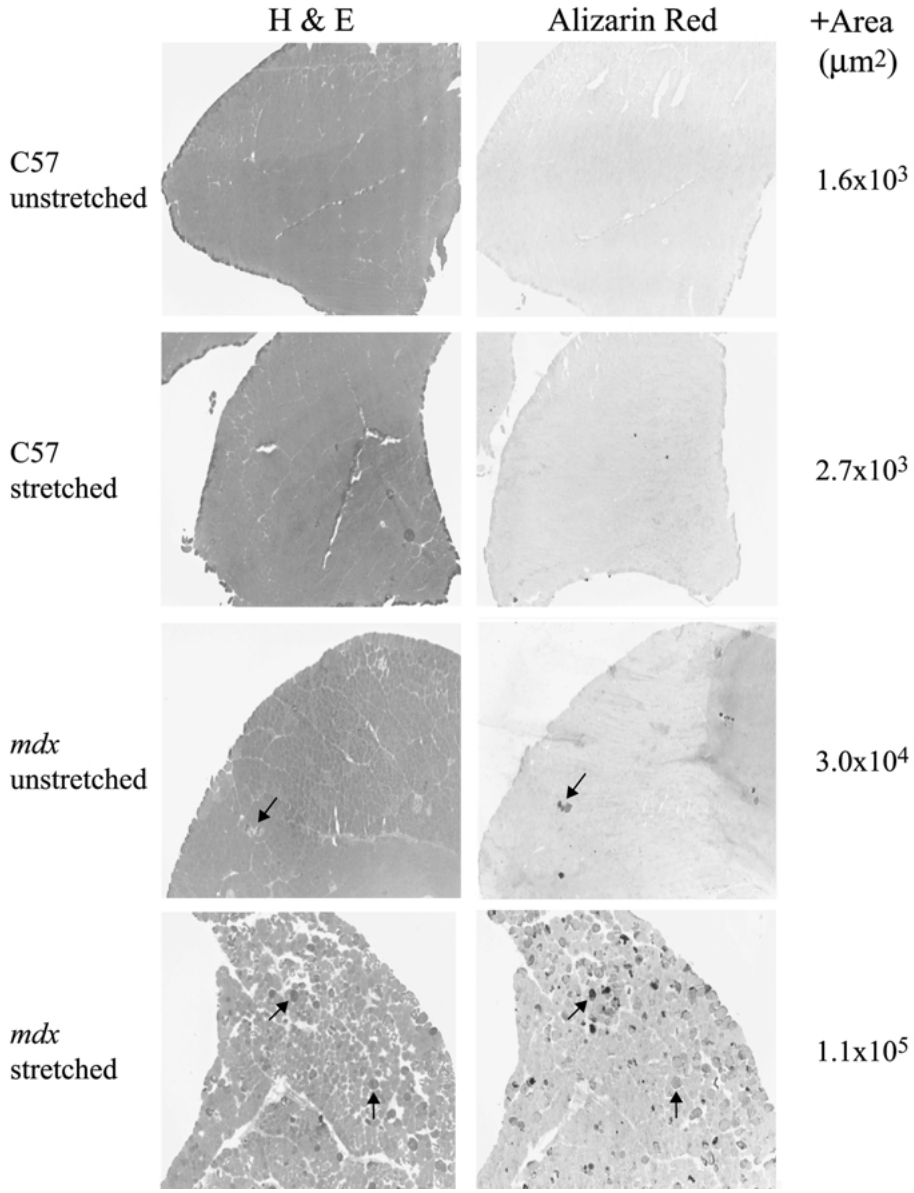

Fig. 5. TA muscles of *mdx* mice subjected to the *in situ* lengthening contraction protocol demonstrated high intracellular calcium. TA muscles from *mdx* and control (C57) mice were subjected to the two-lengthening contraction assay (stretched). The contralateral TA muscle served as the unstretched control. Muscles were frozen in isopentane-cooled liquid nitrogen after a 15-minute recovery period. Serial 5 μm frozen muscle sections were stained with hematoxylin and eosin-phloxine (H&E) or Alizarin red. Shown are images from stained slides photographed at 40× magnification. TA muscles from control mice and unstretched TA muscles from *mdx* mice showed uniform H&E staining and little to no Alizarin red staining. The arrows indicate cells that either appeared necrotic (*mdx* unstretched) or had dark eosin staining (*mdx* stretched) and also stained positive for Alizarin red dye. TA muscles of *mdx* mice that underwent the stretch protocol revealed many darkly stained muscle fibers that were also positive for Alizarin red, demonstrating calcium ion presence inside the cells that likely induced hypercontraction. For quantification of the amount of Alizarin red staining, six 100× microscopic fields were analyzed from muscles of each case (C57 unstretched; $n = 3$ muscles and therefore 18 fields, C57 stretched; $n = 3$, *mdx* unstretched; $n = 4$, *mdx* stretched; $n = 8$). Image Pro Plus calculated the Alizarin red positive area in each field after the image thresholds were adjusted to highlight the red stain and decrease background, with every image treated identically. The average area in a field that was Alizarin red positive for each case is shown (+Area). The total area of a 100× field was 1.4×10^6 μm^2, and was used to calculate the percentage of Alizarin red positive area in a field as described in the results.

for injection studies, the TA muscle has been widely used for such experiments (Gilbert *et al.*, 1999; Greelish *et al.*, 1999; Ebihara *et al.*, 2000; Ferrer *et al.*, 2000; Wakefield *et al.*, 2000; Byun *et al.*, 2001). The four- to seven-fold difference in force deficits between TA muscles in *mdx* and control mice following two 40% lengthening contractions offers an assay for evaluating the efficacy of therapeutic intervention far superior in sensitivity than that provided by either isometric measurements or by morphological evaluations.

The *in situ* assay described in the present study has many advantages in addition to its high sensitivity. The lack of disruption of innervation or blood flow along with the minimally invasive nature of the *in situ* preparation allows for multiple assessments of the muscle over time (Brooks, 1998). In addition, in contrast

to the complexities of whole body exercise, the use of an *in situ* muscle preparation with supramaximal nerve stimulation ensures that every fiber within the muscle is exposed to precisely the same contraction protocol in terms of the level of activation, displacement, and velocity (Faulkner and Brooks, 1994). A further advantage of the assay described in the present study is that, compared with protocols involving many repeated contractions (Sacco *et al*., 1992; Brooks, 1998; Vilquin *et al*., 1998), the two-stretch protocol removes any potential contribution of fatigue to the force deficits measured for these muscles. Finally, the relatively minor injury experienced by control muscles, 8 ± 1% force deficit after the first lengthening contraction and 17 ± 2% after the second supports the use of 40% strain as well within the range of contractions tolerable to TA muscles in cage-reared mice.

The usefulness of any protocol for discriminating between control and dystrophic muscles requires that the effect of the protocol be within a certain range (Gillis, 1999). For protocols that are too benign, muscles in neither *mdx* nor control mice are affected, whereas protocols that are too rigorous overwhelm any difference between dystrophic and control muscles. For TA muscles of *mdx* mice, these two extremes are illustrated by the studies of Brussee *et al*. (1997) and Sacco *et al*. (1992). Brussee showed that TA muscles were relatively unaffected by downhill running with little difference observed between muscles from *mdx* and control mice, whereas Sacco reported virtually equivalent susceptibility to contraction-induced injury of TA muscles from *mdx* and control mice using a rigorous protocol of 240 *in vivo* lengthening contractions. The severe injury induced to control muscles in the study of Sacco *et al*. (1992) suggests that their protocol of 240 lengthening contractions induced maximum injury to muscles of both strains of mice. On the other hand, the lack of TA muscle fiber disruption observed by Brussee *et al*. (1997) likely reflects the relatively non-injurious nature of downhill running to TA muscles (Smith *et al*., 1997). The wide range of force deficits induced by the two-stretch protocol in the present study, from the minor injury experienced by control muscles to the nearly complete inability to generate force of dystrophic muscles, supports the usefulness of this assay for discriminating between the muscles.

Most investigations of muscle injury in *mdx* mice have focused on a single time point in young mice (for review see Gillis, 1999), whereas we examined TA muscles in mice aged 2–19 months. Unlike muscles in control mice, TA muscles of *mdx* mice appear to experience increased susceptibility to contraction-induced injury with age. Head *et al*. (1992) hypothesized that in the muscles of *mdx* mice an elevated susceptibility to damage coincides with the appearance of significant numbers of deformed and abnormally branched muscle fibers, and that the lack of dystrophin may not be solely causal. Abnormally branched fibers may be more susceptible to injury due to atypical stress concentrations associated with the branch points. For EDL muscles of *mdx* mice, a dramatic increase in fiber deformities was observed after 6 months of age (Head *et al*., 1992), roughly the age at which the susceptibility to injury of TA muscles in *mdx* mice in the present study increased substantially. As members of the same functional group with similar fiber type compositions (Burkholder *et al*., 1994), similar abnormalities may be expected to arise in TA and EDL muscles. Structural changes in muscles of *mdx* mice may also contribute to their greater susceptibility to injury through an altered relationship between L_o and L_f. If muscles of *mdx* mice contained relatively shorter fibers than controls, the fibers would be subjected to greater relative strains and consequently damaged more than controls (Brooks *et al*., 1995). However, in this and other studies, no significant differences were observed between *mdx* and control mice for L_o of TA muscles (Sacco *et al*., 1992) or tibial length (Marshall *et al*., 1989).

The mechanism of contraction-induced injury appears to be dramatically different between dystrophic and control muscles (Brooks, 1998), with damage to membranes in dystrophic muscle representing a component of the initial injury that does not occur in control muscles (Petrof *et al*., 1993). Uptake of high molecular weight dyes such as procion orange *in vitro* (Petrof *et al*., 1993) and Evans blue *in vivo* (Matsuda *et al*., 1995; Greelish *et al*., 1999) detect fibers with compromised membrane integrity in dystrophic muscle. In addition, Alizarin red has been used to identify fibers with high intracellular calcium in dystrophic muscles of humans (Bodensteiner and Engel, 1978), canines (Valentine *et al*., 1989, 1990) and hamsters (Greelish *et al*., 1999). Membrane disruption allowing the influx of calcium leading to hypercontraction has been suggested to initiate necrosis in dystrophic fibers (Valentine *et al*., 1989; Matsuda *et al*., 1995). Interestingly, hypercontracted fibers do not generally show primary plasma membrane defects through the uptake of Evans blue dye (Straub *et al*., 1997). In the present study as well, TA muscles in *mdx* mice displayed high levels of intracellular calcium in necrotic fibers (lack of eosin stain), hypercontracted fibers (darkly stained), and normal appearing non-necrotic fibers. Consequently, fibers identified by dye uptake or high calcium may represent separate, but perhaps overlapping, populations (Greelish *et al*., 1999). The increase in the present study in Alizarin red positive area following the stretches of TA muscles of *mdx*, but not control, mice shows that the two-contraction protocol resulted in at least transient muscle fiber membrane damage in the *mdx* mice. Our observation of a significant rapid recovery in force by TA muscles in *mdx*, but not control, mice is also consistent with previous reports of a rapidly recovering component of dystrophic muscle injury hypothesized to be attributable to membrane disruption (Brooks, 1998). The extent to which membrane damage contributed to the inability of muscles in *mdx* mice to generate force (Petrof *et al*., 1993) is not known, but the relatively

small percentage of the cross section that was Alizarin red positive suggests that membrane disruption could not account entirely for the very high force deficits observed.

In conclusion, our assay involving two lengthening contractions of the TA muscle *in situ* allows for immediate evaluation of the magnitude of the injury without fatigue. Immediate evaluation after injury is important to gain a full appreciation of the differences between dystrophic and control muscle. The assay is highly sensitive for detecting differences in *mdx* and control muscles and is even more sensitive in older than younger mice, perhaps due to effects in addition to the lack of dystrophin on susceptibility to injury in older *mdx* mice such as secondary structural changes of fiber splitting or branching. These results are important for therapeutic studies in which mice of varying ages are used to show reversibility, in addition to prevention, of the dystrophic phenotype (Hartigan-O'Connor and Chamberlain, 2000). Even if moderate protection from injury is achieved under the high stress conditions used in this protocol, the usefulness of a corrective therapy aimed at restoring the levels of resistance to contraction-induced injury of control muscles could be demonstrated.

Acknowledgements

We thank John Faulkner and Jeannine Scott for helpful comments on the manuscript. This research was supported by National Institute of Health grants AG-15434 to SVB and JSC and by a grant from the Muscular Dystrophy Association to JSC. CDR was partially supported by a pre-doctoral fellowship from the Rackham Graduate School, University of Michigan.

References

Bodensteiner JB and Engel AG (1978) Intracellular calcium accumulation in Duchenne dystrophy and other myopathies: a study of 567,000 muscle fibers in 114 biopsies. *Neurology* **28:** 439–446.

Brooks SV (1998) Rapid recovery following contraction-induced injury to *in situ* skeletal muscles in *mdx* mice. *J Muscle Res Cell Motil* **19:** 179–187.

Brooks SV, Zerba E and Faulkner JA (1995) Injury to muscle fibres after single stretches of passive and maximally stimulated muscles in mice. *J Physiol (Lond)* **488:** 459–469.

Brussee V, Tardif F and Tremblay JP (1997) Muscle fibers of *mdx* mice are more vulnerable to exercise than those of normal mice. *Neuromuscul Disord* **7:** 487–492.

Bulfield G, Siller WG, Wight PA and Moore KJ (1984) X chromosome-linked muscular dystrophy (*mdx*) in the mouse. *Proc Natl Acad Sci USA* **81:** 1189–1192.

Burkholder TJ, Fingado B, Baron S and Lieber RL (1994) Relationship between muscle fiber types and sizes and muscle architectural properties in the mouse hindlimb. *J Morphol* **221:** 177–190.

Byun J, Heard JM, Huh JE, Park SJ, Jung EA, Jeong JO, Gwon HC and Kim DK (2001) Efficient expression of the vascular endothelial growth factor gene *in vitro* and *in vivo*, using an adeno-associated virus vector. *J Mol Cell Cardiol* **33:** 295–305.

Cox GA, Cole NM, Matsumura K, Phelps SF, Hauschka SD, Campbell KP, Faulkner JA and Chamberlain JS (1993) Overexpression of dystrophin in transgenic *mdx* mice eliminates dystrophic symptoms without toxicity. *Nature* **364:** 725–729.

Deconinck N, Rafael JA, Beckers-Bleukx G, Kahn D, Deconinck AE, Davies KE and Gillis JM (1998) Consequences of the combined deficiency in dystrophin and utrophin on the mechanical properties and myosin composition of some limb and respiratory muscles of the mouse. *Neuromuscul Disord* **8:** 362–370.

Dubowitz V (1985) *Muscle Biopsy: A practical approach*. Bailliere Tindall Ltd., London.

Ebihara S, Guibinga GH, Gilbert R, Nalbantoglu J, Massie B, Karpati G and Petrof BJ (2000) Differential effects of dystrophin and utrophin gene transfer in immunocompetent muscular dystrophy (*mdx*) mice. *Physiol Genom* **3:** 133–144.

Emery AEH (1993) *Duchenne Muscular Dystrophy*. Oxford Medical Publications, Oxford.

Faulkner JA and Brooks SV (1994) An *in situ* single skeletal muscle model of contraction-induced injury: mechanistic interpretations. *Basic Appl Myol* **4:** 17–23.

Faulkner JA, Brooks SV, Dennis RG and Lynch GS (1997) The functional status of dystrophic muscles and functional recovery by skeletal muscles following myoblast transfer. *Basic Appl Myol* **7:** 257–264.

Ferrer A, Wells KE and Wells DJ (2000) Immune responses to dystropin: implications for gene therapy of Duchenne muscular dystrophy. *Gene Ther* **7:** 1439–1446.

Gilbert R, Nalbantoglu J, Petrof BJ, Ebihara S, Guibinga GH, Tinsley JM, Kamen A, Massie B, Davies KE and Karpati G (1999) Adenovirus-mediated utrophin gene transfer mitigates the dystrophic phenotype of *mdx* mouse muscles. *Hum Gene Ther* **10:** 1299–1310.

Gillis JM (1999) Understanding dystrophinopathies: an inventory of the structural and functional consequences of the absence of dystrophin in muscles of the *mdx* mouse. *J Muscle Res Cell Motil* **20:** 605–625.

Greelish JP, Su LT, Lankford EB, Burkman JM, Chen H, Konig SK, Mercier IM, Desjardins PR, Mitchell MA, Zheng XG, Leferovich J, Gao GP, Balice-Gordon RJ, Wilson JM and Stedman HH (1999) Stable restoration of the sarcoglycan complex in dystrophic muscle perfused with histamine and a recombinant adeno-associated viral vector. *Nat Med* **5:** 439–443.

Hartigan-O'Connor D and Chamberlain JS (2000) Developments in gene therapy for muscular dystrophy. *Microsc Res Tech* **48:** 223–238.

Head SI, Williams DA and Stephenson DG (1992) Abnormalities in structure and function of limb skeletal muscle fibres of dystrophic *mdx* mice. *Proc R Soc Lond B Biol Sci* **248:** 163–169.

Hoffman EP, Brown RH Jr and Kunkel LM (1987) Dystrophin: the protein product of the Duchenne muscular dystrophy locus. *Cell* **51:** 919–928.

Lynch GS, Hinkle RT, Chamberlain JS, Brooks SV and Faulkner JA (2001) Force output of fast and slow skeletal muscles from young, adult and old *mdx* mice. *J Physiol London* **535:** 591–600.

Lynch GS, Rafael JA, Chamberlain JS and Faulkner JA (2000) Contraction-induced injury to single permeabilized muscle fibers from *mdx*, transgenic *mdx*, and control mice. *Am J Physiol Cell Physiol* **279:** C1290–C1294.

Marshall PA, Williams PE and Goldspink G (1989) Accumulation of collagen and altered fiber-type ratios as indicators of abnormal muscle gene expression in the *mdx* dystrophic mouse. *Muscle Nerve* **12:** 528–537.

Matsuda R, Nishikawa A and Tanaka H (1995) Visualization of dystrophic muscle fibers in *mdx* mouse by vital staining with Evans blue: evidence of apoptosis in dystrophin-deficient muscle. *J Biochem (Tokyo)* **118:** 959–964.

Mendez J and Keys A (1960) Density and composition of mammalian muscle. *Metabolism* **9:** 184–188.

Moens P, Baatsen PH and Marechal G (1993) Increased susceptibility of EDL muscles from *mdx* mice to damage induced by contractions with stretch. *J Muscle Res Cell Motil* **14:** 446–451.

Petrof BJ, Shrager JB, Stedman HH, Kelly AM and Sweeney HL (1993) Dystrophin protects the sarcolemma from stresses devel-

oped during muscle contraction. *Proc Natl Acad Sci USA* **90:** 3710–3714.

Phelps SF, Hauser MA, Cole NM, Rafael JA, Hinkle RT, Faulkner JA and Chamberlain JS (1995) Expression of full-length and truncated dystrophin mini-genes in transgenic *mdx* mice. *Hum Mol Genet* **4:** 1251–1258.

Sacco P, Jones DA, Dick JR and Vrbova G (1992) Contractile properties and susceptibility to exercise-induced damage of normal and *mdx* mouse tibialis anterior muscle. *Clin Sci (Colch)* **82:** 227–236.

Sicinski P, Geng Y, Ryder-Cook AS, Barnard EA, Darlison MG and Barnard PJ (1989) The molecular basis of muscular dystrophy in the *mdx* mouse: a point mutation. *Science* **244:** 1578–1580.

Smith HK, Plyley MJ, Rodgers CD and McKee NH (1997) Skeletal muscle damage in the rat hindlimb following single or repeated daily bouts of downhill exercise. *Int J Sports Med* **18:** 94–100.

Stedman HH, Sweeney HL, Shrager JB, Maguire HC, Panettieri RA, Petrof B, Narusawa M, Leferovich JM, Sladky JT and Kelly AM (1991) The *mdx* mouse diaphragm reproduces the degenerative changes of Duchenne muscular dystrophy. *Nature* **352:** 536–539.

Straub V, Rafael JA, Chamberlain JS and Campbell KP (1997) Animal models for muscular dystrophy show different patterns of sarcolemmal disruption. *J Cell Biol* **139:** 375–385.

Valentine BA, Cooper BJ and Gallagher EA (1989) Intracellular calcium in canine muscle biopsies. *J Compar Pathol* **100:** 223–230.

Valentine BA, Cooper BJ, Cummings JF and de Lahunta A (1990) Canine X-linked muscular dystrophy: morphologic lesions. *J Neurol Sci* **97:** 1–23.

Vilquin JT, Brussee V, Asselin I, Kinoshita I, Gingras M and Tremblay JP (1998) Evidence of *mdx* mouse skeletal muscle fragility *in vivo* by eccentric running exercise. *Muscle Nerve* **21:** 567–576.

Wakefield PM, Tinsley JM, Wood MJ, Gilbert R, Karpati G and Davies KE (2000) Prevention of the dystrophic phenotype in dystrophin/utrophin-deficient muscle following adenovirus-mediated transfer of a utrophin minigene. *Gene Ther* **7:** 201–204.